Characterization and analysis of timing jitter in normal-dispersion mode-locked Er-fiber lasers with intra-cavity filtering

Junho Shin,[1] Kwangyun Jung,[1] Youjian Song,[2] and Jungwon Kim[1,*]

[1]*Korea Advanced Institute of Science and Technology (KAIST), Daejeon 305-701, South Korea*
[2]*School of Precision Instrument and Optoelectronics Engineering, Tianjin University, Tianjin 300072, China*
**jungwon.kim@kaist.ac.kr*

Abstract: We characterize and analyze the timing jitter of normal-dispersion mode-locked Er-fiber lasers with intra-cavity filtering. The timing jitter of Er-fiber lasers with 9-nm bandpass filters operating at + 0.0084 ps^2 is measured to be 3.46 fs (rms) when integrated from 10 kHz to 10 MHz offset frequency, which is similar to the jitter level of typical stretched-pulse or soliton Er-fiber lasers. The numerical simulation based on split-step Fourier transform method shows that the measured high-frequency jitter is quantum noise-limited performance. We also develop an analytical model for filtered normal-dispersion fiber lasers by modifying the well-established noise model of stretched-pulse fiber lasers. The analytical modeling reveals that the jitter performance is improved mostly by reducing the chirp parameter by intra-cavity filtering. Both numerical simulation and analytical model fit fairly well with the measured timing jitter result.

OCIS codes: (320.7090) Ultrafast lasers; (270.2500) Fluctuations, relaxations, and noise; (140.4050) Mode-locked lasers.

References and links

1. R. K. Shelton, S. M. Foreman, L. S. Ma, J. L. Hall, H. C. Kapteyn, M. M. Murnane, M. Notcutt, and J. Ye, "Subfemtosecond timing jitter between two independent, actively synchronized, mode-locked lasers," Opt. Lett. **27**(5), 312–314 (2002).
2. T. R. Schibli, J. Kim, O. Kuzucu, J. T. Gopinath, S. N. Tandon, G. S. Petrich, L. A. Kolodziejski, J. G. Fujimoto, E. P. Ippen, and F. X. Kaertner, "Attosecond active synchronization of passively mode-locked lasers by balanced cross correlation," Opt. Lett. **28**(11), 947–949 (2003).
3. J. J. McFerran, E. N. Ivanov, A. Bartels, G. Wilpers, C. W. Oates, S. A. Diddams, and L. Hollberg, "Low-noise synthesis of microwave signals from an optical source," Electron. Lett. **41**(11), 650–651 (2005).
4. J. Kim, J. A. Cox, J. Chen, and F. X. Kartner, "Drift-free femtosecond timing synchronization of remote optical and microwave sources," Nat. Photonics **2**(12), 733–736 (2008).
5. G. C. Valley, "Photonic analog-to-digital converters," Opt. Express **15**(5), 1955–1982 (2007).
6. F. Quinlan, T. M. Fortier, M. S. Kirchner, J. A. Taylor, M. J. Thorpe, N. Lemke, A. D. Ludlow, Y. Jiang, and S. A. Diddams, "Ultralow phase noise microwave generation with an Er:fiber-based optical frequency divider," Opt. Lett. **36**(16), 3260–3262 (2011).
7. K. Jung, J. Shin, and J. Kim, "Ultralow phase noise microwave generation from mode-locked Er-fiber lasers with subfemtosecond integrated timing jitter," IEEE Photonics J. **5**(3), 5500906 (2013).
8. P. Ghelfi, F. Laghezza, F. Scotti, G. Serafino, A. Capria, S. Pinna, D. Onori, C. Porzi, M. Scaffardi, A. Malacarne, V. Vercesi, E. Lazzeri, F. Berizzi, and A. Bogoni, "A fully photonics-based coherent radar system," Nature **507**(7492), 341–345 (2014).
9. G. A. Keeler, B. E. Nelson, D. Agarwal, C. Debaes, N. C. Helman, A. Bhatnagar, and D. A. B. Miller, "The benefits of ultrashort optical pulses in optically interconnected systems," IEEE J. Sel. Top. Quantum Electron. **9**(2), 477–485 (2003).
10. Y. Song, C. Kim, K. Jung, H. Kim, and J. Kim, "Timing jitter optimization of mode-locked Yb-fiber lasers toward the attosecond regime," Opt. Express **19**(15), 14518–14525 (2011).
11. T. K. Kim, Y. Song, K. Jung, C. Kim, H. Kim, C. H. Nam, and J. Kim, "Sub-100-as timing jitter optical pulse trains from mode-locked Er-fiber lasers," Opt. Lett. **36**(22), 4443–4445 (2011).
12. L. A. Jiang, M. E. Grein, E. P. Ippen, C. McNeilage, J. Searls, and H. Yokoyama, "Quantum-limited noise performance of a mode-locked laser diode," Opt. Lett. **27**(1), 49–51 (2002).

#243785 Received 25 Jun 2015; revised 19 Aug 2015; accepted 19 Aug 2015; published 21 Aug 2015

13. C. Ouyang, P. Shum, H. Wang, J. H. Wong, K. Wu, S. Fu, R. Li, E. J. R. Kelleher, A. I. Chernov, and E. D. Obraztsova, "Observation of timing jitter reduction induced by spectral filtering in a fiber laser mode locked with a carbon nanotube-based saturable absorber," Opt. Lett. **35**(14), 2320–2322 (2010).
14. O. Prochnow, R. Paschotta, E. Benkler, U. Morgner, J. Neumann, D. Wandt, and D. Kracht, "Quantum-limited noise performance of a femtosecond all-fiber ytterbium laser," Opt. Express **17**(18), 15525–15533 (2009).
15. P. Qin, Y. Song, H. Kim, J. Shin, D. Kwon, M. Hu, C. Wang, and J. Kim, "Reduction of timing jitter and intensity noise in normal-dispersion passively mode-locked fiber lasers by narrow band-pass filtering," Opt. Express **22**(23), 28276–28283 (2014).
16. J. P. Gordon and H. A. Haus, "Random walk of coherently amplified solitons in optical fiber transmission," Opt. Lett. **11**(10), 665–667 (1986).
17. P. Grelu and N. Akhmediev, "Dissipative solitons for mode-locked lasers," Nat. Photonics **6**(2), 84–92 (2012).
18. J. A. Cox, A. H. Nejadmalayeri, J. Kim, and F. X. Kärtner, "Complete characterization of quantum-limited timing jitter in passively mode-locked fiber lasers," Opt. Lett. **35**(20), 3522–3524 (2010).
19. C. Kim, K. Jung, K. Kieu, and J. Kim, "Low timing jitter and intensity noise from a soliton Er-fiber laser mode-locked by a fiber taper carbon nanotube saturable absorber," Opt. Express **20**(28), 29524–29530 (2012).
20. S. Namiki and H. Haus, "Noise of the stretched pulse fiber laser: I. Theory," IEEE J. Quantum Electron. **33**(5), 649–659 (1997).
21. G. P. Agrawal, *Nonlinear Fiber Optics* (Academic Press, 2006).
22. K. Jung and J. Kim, "Characterization of timing jitter spectra in free-running mode-locked lasers with 340 dB dynamic range over 10 decades of Fourier frequency," Opt. Lett. **40**(3), 316–319 (2015).
23. R. P. Scott, C. Langrock, and B. H. Kolner, "High-dynamic-range laser amplitude and phase noise measurement techniques," IEEE J. Sel. Top. Quantum Electron. **7**(4), 641–655 (2001).
24. R. Paschotta, "Noise of mode-locked lasers (Part II): timing jitter and other fluctuations," Appl. Phys. B **79**(2), 163–173 (2004).
25. H. A. Haus, "Quantum noise in a solitonlike repeater system," J. Opt. Soc. Am. B **8**(5), 1122–1126 (1991).
26. R. Paschotta, "Timing jitter and phase noiseof mode-locked fiber lasers," Opt. Express **18**(5), 5041–5054 (2010).

1. Introduction

Ultralow timing jitter femtosecond mode-locked lasers can be used for timing synchronization [1–4], optical sampling and analog-to-digital conversion [5], low-noise microwave generation [3,6,7], photonic radars [8], and optical interconnection [9], to name a few. In particular, mode-locked fiber lasers have attracted attention due to their advantages of simpler design and implementation, better robustness and lower cost, compared to solid-state bulk lasers. Previous research on lower jitter fiber lasers has been mainly focused on dispersion engineering. Operating stretched-pulse, nonlinear polarization evolution (NPE)-based fiber lasers at close-to-zero dispersion has enabled the scaling of high-frequency (e.g., >10 kHz offset frequency) timing jitter to the sub-femtosecond regime [10,11]. However, timing jitter of stretched-pulse fiber lasers is highly sensitive to the net cavity dispersion including higher-order dispersion. In addition, even at the same dispersion condition, depending on the input polarization states and mode-locking condition, timing jitter spectra can vary more than 10 dB as shown in [10]. Due to these issues, reduction of timing jitter by dispersion engineering in stretched-pulse fiber lasers is nontrivial.

Recently, timing jitter reduction by intra-cavity filtering in mode-locked lasers has been a topic of interest [12–15]. It has been well known that narrow bandpass filtering can reduce the timing jitter originated from the quantum-limited center frequency noise coupled via dispersion (also called the Gordon-Haus jitter) [16]. In a hybrid-mode-locked semiconductor laser, it was shown that the timing jitter could be reduced from 1.7 ps to 86 fs by employing a 0.7-nm bandpass filter in the cavity [12]. It was also shown that the timing jitter in soliton mode-locked Er-fiber lasers could be reduced from 84.8 fs to 29.1 fs by intra-cavity filtering [13]. The timing jitter of all-fiber, normal-dispersion Yb-laser with 9-nm bandpass filter was measured to be 90 fs when integrated from 100 Hz to 10 kHz offset frequency [14]. More recently, systematic measurements of normal-dispersion Yb-fiber lasers at different intra-cavity dispersion and filter conditions revealed that timing jitter becomes nearly independent of intra-cavity dispersion when inserting a narrow bandpass filter in normal-dispersion fiber lasers [15]. Further, it was shown that high-frequency (>10 kHz) timing jitter could reach the sub-femtosecond regime by narrow intra-cavity filtering. Combining these experimental findings with the high stability and reproducibility of dissipative soliton solution [17], intra-cavity filtering in a normal-dispersion Er-fiber laser may lead to a more robust and higher

#243785 Received 25 Jun 2015; revised 19 Aug 2015; accepted 19 Aug 2015; published 21 Aug 2015

energy optical pulse train generator with femtosecond timing jitter at telecommunication wavelength.

In this paper, we show the accurate timing jitter measurement result of normal-dispersion (+ 0.0084 ps^2) Er-fiber lasers with 9-nm intra-cavity filtering. The measured timing jitter is 3.46 fs (rms) when integrated from 10 kHz to 10 MHz offset frequency, which is similar to the timing jitter in typical stretched-pulse Er-fiber lasers [18] or all-fiber soliton Er lasers [19]. Further, based on accurate measurement of timing jitter spectral density and associated laser parameters, we analyze the jitter spectrum using both numerical simulations and analytical modeling. The numerical simulation based on split-step Fourier transform method shows that the measured jitter above 10 kHz offset frequency is quantum noise-limited performance. We also develop an analytical model for filtered normal-dispersion fiber lasers by modifying the Namiki-Haus noise model for stretched-pulse fiber lasers [20]. The analysis result suggests that the jitter performance is improved mostly by reducing the chirp parameter by intra-cavity filtering. Both numerical simulation and analytical model fit fairly well with the measured results when setting the spontaneous emission factor (excess noise factor) at three.

2. Design and implementation of normal-dispersion Er-fiber lasers with intra-cavity filtering

Figure 1(a) shows the schematic of the implemented normal-dispersion Er-fiber laser with an intra-cavity bandpass filter. Mode-locking of the laser is achieved by NPE. The used gain fiber is 60 cm of high-concentration Er-doped fiber (ER-110-4/125, Liekki). Passive fiber section consists of a wavelength division multiplexer (OFS980-16, OFS) and a section of small-core fiber (HI1060, Corning). Polarization components (wave-plates and polarization beam splitter), a spectral filter, and an isolator are placed in the free-space section. The used spectral filter is a standard off-the-shelf product (NIR01-1550/3-25, Semrock) and has a flattop pass-band shape with ~9 nm full width half maximum (FWHM) bandwidth at 1550 nm center wavelength. To overcome the filtering loss, two pump laser diodes (1999CHP, 3SP Group) at 980 nm are used through the pump beam combiner. The laser is forward-pumped for lower noise, and the combined pump power is about 1 W. The length of the passive fiber section is optimized to achieve enough spectral broadening while preventing the pulse breaking. The length of the passive fiber after gain section is 45 cm, while 30 cm of passive fiber is used before the gain fiber. With the known dispersion values of Er (+ 12 fs^2/mm) and passive (–6.6 fs^2/mm for HI1060, + 4.5 fs^2/mm for OFS980-16) fibers, the net cavity dispersion is about + 0.0084 ps^2 at 1550 nm. The laser is implemented as a sigma cavity with a mirror mounted on a piezoelectric transducer (PZT) for easy repetition-rate locking.

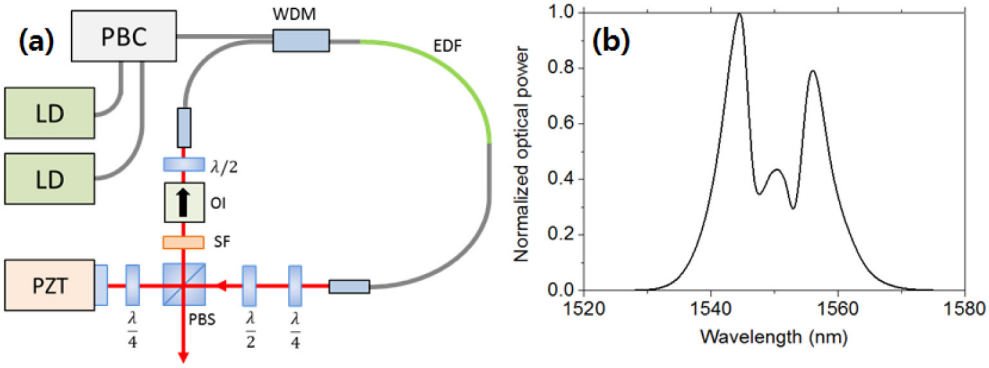

Fig. 1. (a) Schematic of the filtered normal-dispersion Er-fiber laser. (b) Measured output optical spectrum. EDF, erbium-doped fiber; LD, laser diode; OI, optical isolator; PBC, pump beam combiner; PBS, polarization beam splitter; PZT, piezoelectric transducer; SF, spectral filter; WDM, wavelength division multiplexer.

#243785 Received 25 Jun 2015; revised 19 Aug 2015; accepted 19 Aug 2015; published 21 Aug 2015

By adjusting the waveplates, stable and robust mode-locking can be obtained. The average output power is ~145 mW, and the repetition-rate is 129 MHz. The FWHM pulse width at the output coupler is ~620 fs, which is measured by an intensity auto-correlator. The measured optical spectrum from the output coupler is shown in Fig. 1(b). The FWHM bandwidth is 17 nm, and the multi-peak profile of the spectrum is the result of self-phase modulation (SPM) [21]. From the shape of the optical spectrum, the accumulated nonlinear phase shift is estimated to be ~1.2π rad. The radio-frequency (RF) spectra of the pulse train are shown in Fig. 2. The measured signal-to-noise ratio (SNR) is >80 dB for 10-Hz resolution bandwidth [Fig. 2(a)]. The broadband RF spectrum over 1 GHz span shows stable fundamental mode-locking without sign of multi-pulsing or wave-breaking [Fig. 2(b)].

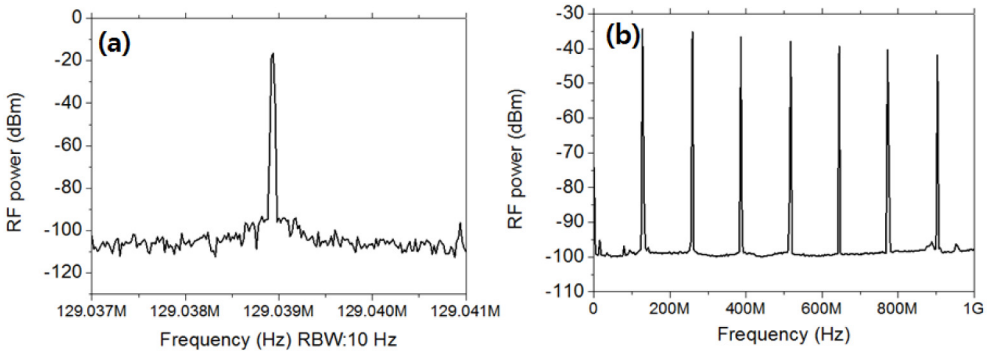

Fig. 2. RF spectrum (a) with resolution bandwidth of 10 Hz, (b) with frequency span of 1 GHz.

3. Measurement results of relative intensity noise and timing jitter

To check the power stability of the laser, relative intensity noise (RIN) is measured with and without a 9-nm bandpass filter, and its result is shown in Fig. 3. The RIN suppression by spectral filtering is observed for normal-dispersion Er-fiber laser, as was also shown in Yb-fiber lasers in [15]. Note that multiple peaks in the 10 Hz – 1 kHz are mainly caused by the acoustic noise, mechanical vibrations and 60-Hz AC power lines, and their strength strongly depends on the laboratory environment. The integrated RIN for the filtered case is 0.0047% (rms) when integrated from 10 Hz to 100 kHz, while the integrated RIN without the filter is 0.033% with the same integration range.

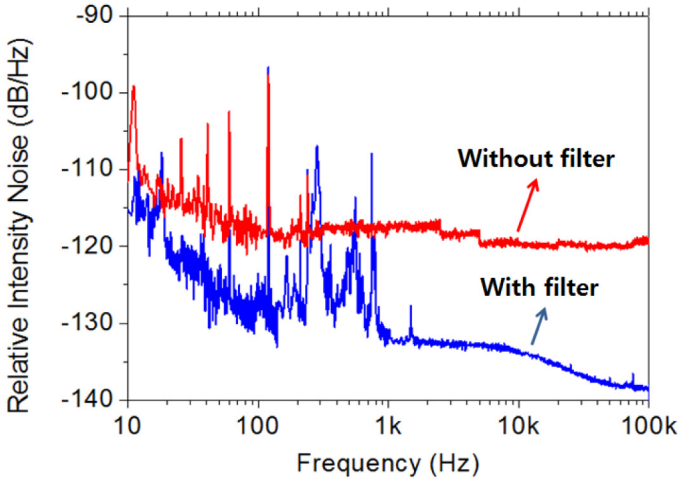

Fig. 3. Reduction of RIN by intra-cavity filtering.

#243785 Received 25 Jun 2015; revised 19 Aug 2015; accepted 19 Aug 2015; published 21 Aug 2015

The experimental setup for timing jitter measurement is shown in Fig. 4. To measure the timing jitter of the laser-under-test (Laser 1 in Fig. 4), we need an additional reference laser (Laser 2 in Fig. 4) with timing jitter equal to or lower than that of the laser-under-test. Therefore, we constructed two almost identical Er-fiber lasers as described in Section 2. The measurement is performed by a well-established, sub-100-attosecond-resolution balanced optical cross-correlation (BOC) method [2]. For the BOC measurement, the outputs from two lasers are combined with orthogonal polarization states. The BOC uses type-II phase-matched second harmonic generation (SHG) by PPKTP with 46.2 μm period. The used balanced detector is a home-made one with trans-impedance gain of 31 kΩ, bandwidth of 44 MHz, and responsivity of 0.53 A/W. The S-curve generated from the balanced detector is used for the phase-locked loop (PLL) between the two free-running fiber lasers. The PLL consists of proportional-integral (PI) servo (LB1005, Newfocus), pre-amplifier (SR560, Stanford Research Systems), and high-voltage amplifier (A-301HS, A.A. Lab Systems). Once the repetition-rate locking between the lasers is obtained, timing jitter above locking bandwidth can be measured directly at the BOC output. The timing jitter below the locking bandwidth can be further extracted by measuring the voltage noise at the PI servo output (input to the PZT amplifier). This voltage noise carries the frequency noise information, which can be converted to the equivalent timing jitter and repetition-rate phase noise. Once the timing jitter spectral density is measured, the measured jitter spectrum is divided by two, assuming that each fiber laser is independent and has equal contribution to the total jitter spectrum [18]. More detailed information on the measurement set-up and timing jitter conversion method can be found in [22].

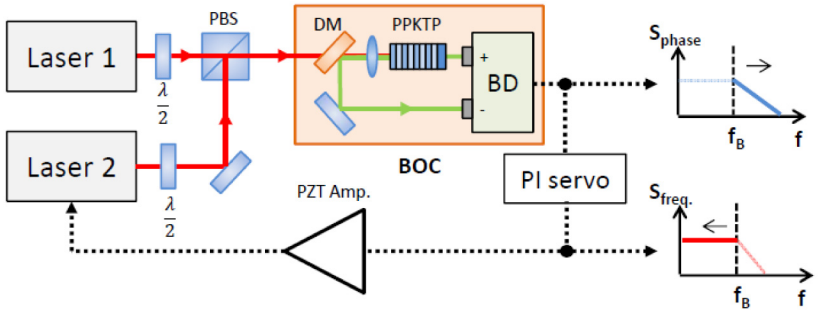

Fig. 4. Experimental setup for timing jitter measurement with the BOC. BD, balanced detector; DM, dichoric mirror; PBS, polarization beam splitter; PI, proportional-integral controller. f_B denotes the PLL locking bandwidth.

To compare the timing jitter between lasers with and without intra-cavity filtering, the same experiment can be performed after removing 9-nm filters from both lasers. However, without narrow intra-cavity filtering, we had a difficulty in obtaining stable mode-locking at large normal (~ + 0.01 ps^2) net-cavity dispersion. As a result, we could operate only one laser without intra-cavity filtering. To measure the timing jitter of this filter-less laser, instead of the BOC method, we apply a standard direct photodetection method [23]: 1.29-GHz (10th harmonic) microwave signal is generated from the mode-locked laser via high-speed photodetection and narrow bandpass filtering at 1.29 GHz. The phase noise of this microwave signal can be obtained by frequency-mixing it in quadrature with 1.29-GHz signal generated from a low-noise microwave synthesizer. Despite a limited measurement dynamic range, we could compare the jitter performance between lasers with and without intra-cavity filtering for <20 kHz offset frequency range.

The measured timing jitter spectral density is shown in Fig. 5. For the laser with intra-cavity filtering (curve (a) in Fig. 5), the jitter spectrum above 4 kHz offset frequency is obtained by directly analyzing the BOC output; the jitter spectrum below 4 kHz offset frequency is obtained by converting the frequency noise at the PZT amplifier input to the equivalent timing jitter. For >10 kHz offset frequency, the measured jitter spectrum slope

#243785 Received 25 Jun 2015; revised 19 Aug 2015; accepted 19 Aug 2015; published 21 Aug 2015

shows −20 dB/decade, which implies the random walk nature of the quantum-limited noise. After the transition range of −30 dB/decade slope in the 1 kHz – 10 kHz, the jitter spectrum in the 10 Hz – 1 kHz shows −20 dB/decade slope again. Many noise peaks in the 100 Hz – 1 kHz are due to the acoustic noise coupling, which are mainly caused by the fan noise of instruments in the laboratory. Below 10 Hz offset frequency, the timing jitter slope rapidly increases to > −50 dB/decade, which is also observed for stretched-pulse fiber lasers [22]. The integrated timing jitter is 3.46 fs (rms) when integrated from 10 kHz to 10 MHz offset frequency. This jitter number is fairly low, corresponding to a similar level with that of stretched-pulse Er-fiber laser operating at positive dispersion (net-cavity dispersion = + 0.004 ps^2) [18] or all-fiber soliton Er-laser mode-locked by a carbon nanotube saturable absorber (net-cavity dispersion = −0.055 ps^2) [19]. Note that the 9-nm bandwidth is used in the experiment because this filter was the only off-the-shelf product that we could easily purchase at the time of experiment. It will be possible to further reduce the jitter by using different filter bandwidths as shown in [15]. When comparing the jitter spectrum between lasers with and without intra-cavity filtering (curve (b) in Fig. 5), the filtered laser has ~20 dB lower jitter spectrum at 10 kHz offset frequency, which shows the effectiveness of narrow intra-cavity filtering for suppressing timing jitter. Note that the measurement resolution of direct photodetection method is limited by the thermal noise floor above 20 kHz offset frequency (dashed line (c) in Fig. 5).

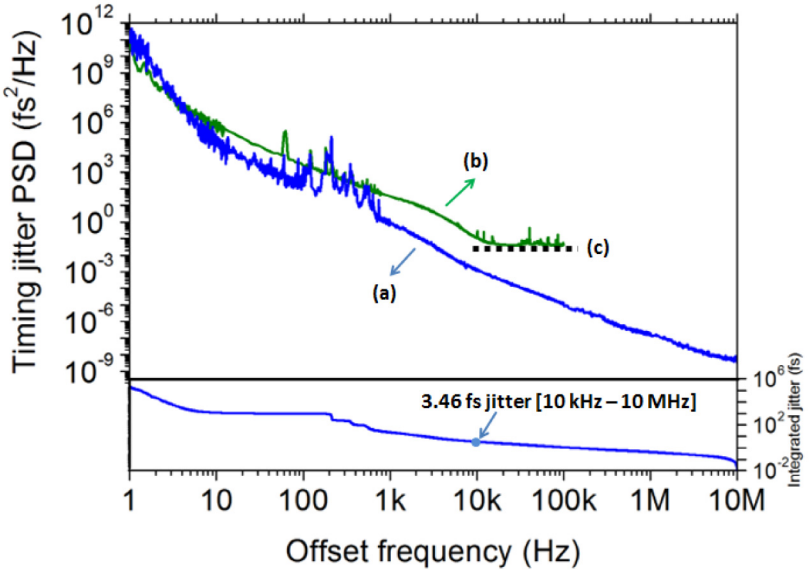

Fig. 5. Measured timing jitter power spectral density and integrated timing jitter of normal-dispersion Er-fiber laser (a) with and (b) without intra-cavity filtering. Note that timing jitter of filtered laser is measured by the BOC whereas timing jitter of filter-less laser is measured by direct photodetection and microwave mixer, which caused the measurement resolution floor above 20 kHz offset frequency (dashed line (c)).

4. Numerical simulation and analytical modeling of the measured timing jitter spectrum

4.1. Numerical simulation of timing jitter

For the numerical analysis of timing jitter in normal-dispersion fiber laser with intra-cavity filtering, we construct a numerical fiber cavity model. The used dispersion values at 1550 nm are + 0.012 ps^2/m for Er fiber, + 0.0045 ps^2/m for OFS980-16 fiber, and −0.0066 ps^2/m for HI1060 fiber. Note that only the second-order dispersion of the fiber is used for the model while higher-order dispersion is not included. The output coupling ratio of ~85% is used for

#243785 Received 25 Jun 2015; revised 19 Aug 2015; accepted 19 Aug 2015; published 21 Aug 2015

model, which is a measured value by inserting the glass plate in the actual laser. The NPE is modeled as an ideal fast saturable absorber in the simulation. In addition, the small signal gain and the gain saturation energy are adjusted in the simulation to match the output pulse energy measured in the experiment. The pulse dynamics in the laser cavity is reconstructed by the well-established split-step Fourier transform (SSFT) method [21]. The laser operation is modeled as a successive propagation of many round-trips in a fiber cavity. To calculate the pulse width in the cavity, the time space of 3 ps span with 4096 segments are used with a rectangular window. Since the pulse width is less than 1 ps, the rectangular window raises no numerical artifact. The time interval between each segment is about 0.7 fs, which allows femtosecond-resolution pulse width analysis. To analyze the optical spectrum, the time span of window is changed from 3 ps to 160 ps while keeping the number of segments identical. The initial pulse is a Gaussian pulse and its pulse energy is matched to the measured pulse energy. The simulation converges to the steady-state after ~450 cycles with 10^{-16}–level relative instability.

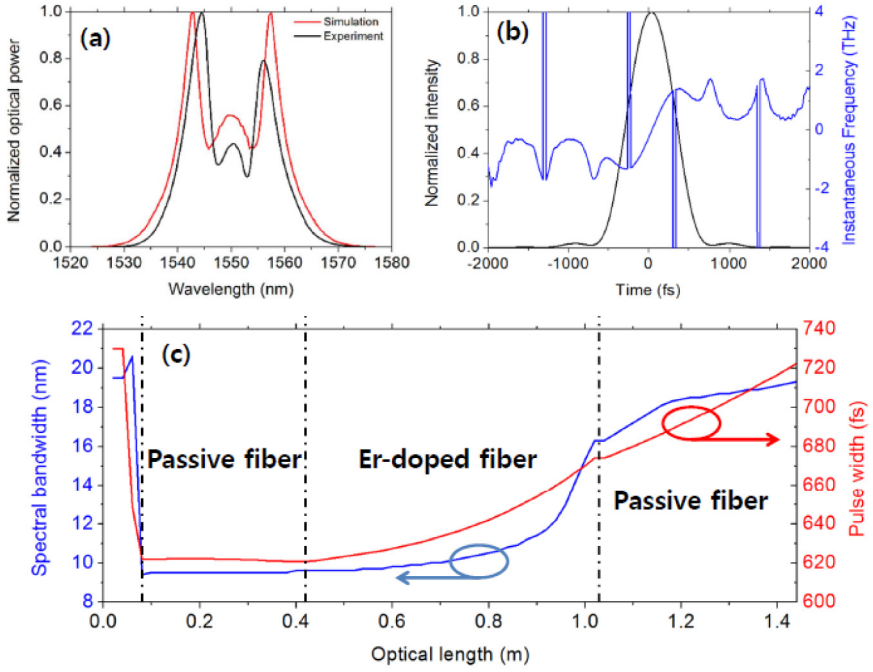

Fig. 6. (a) Optical spectra from the numerical and experimental results. (b) Pulse shape and chirp from numerical analysis. (c) Pulse width and spectrum evolution in the cavity.

The main results of the pulse dynamics simulation are summarized in Fig. 6. Figure 6(a) shows the optical spectra of the numerical simulation and actual measurement results. The numerical result is fairly consistent with the measurement result. Slight differences are due to the assumption of completely symmetric gain spectrum with 45-nm bandwidth Gaussian spectrum profile in the model. From the simulation, the nonlinear phase shift is calculated as 1.1π, of which ~60% is accumulated in the gain medium. Due to the shorter fiber length and smaller total dispersion, the nonlinear phase shift amount is smaller compared to that of typical normal-dispersion lasers mostly intended for power scaling. Note that shorter fiber length is desirable for improving the timing jitter due to shorter pulse width in the gain medium [24]. Figure 6(b) shows the numerically computed pulse shape at the output coupler, which shows ~660 fs FWHM pulse width. Figure 6(c) shows the pulse dynamics in the fiber cavity. As expected, both the pulse width and the optical bandwidth increase during fiber propagation, and are reduced by spectral filtering.

#243785 Received 25 Jun 2015; revised 19 Aug 2015; accepted 19 Aug 2015; published 21 Aug 2015

After making sure that the numerical simulation of pulse dynamics can effectively reproduce the measured laser parameters (such as pulsewidth, output power, spectral shape and bandwidth), we attempted the numerical computation of timing jitter spectral density from this model. To calculate the quantum-limited timing jitter of a mode-locked laser, we introduce the ASE noise in the gain fiber. The introduced ASE quantum noise is white noise described as $\overline{\tilde{n}^*(z,\Omega)\tilde{n}(z',\Omega)} = \frac{1}{2\pi}\frac{1}{\Omega^2/\Delta\omega_g^2+1}\frac{\theta(G-1)}{l}\delta(z-z')\delta(\Omega-\Omega')$, where $\tilde{n}$ is noise, $\tilde{n}^*$ is complex conjugate of noise, G is net power gain, l is length of gain medium, θ is spontaneous emission factor (excess noise factor), z is position of the noise source, Ω is deviation from the carrier frequency, $\Delta\omega_g$ is bandwidth of the amplifier, and δ is delta function [25]. The introduced quantum noise spectrum is converted to the white Gaussian noise electric field and added to the pulse electric field: addition of noisy electric field changes the pulse shape, energy, and temporal position in a random way. The optical pulse train is numerically dithered with the aforementioned quantum noise in the gain medium. After the timing deviation over 200,000 cycles is calculated, it is Fourier-transformed to the power spectral density. For reliable result, total cycles are divided into 8 segments, and each segment contains 25,000 pulses. Given that the repetition-rate is 129 MHz, each segment contains the jitter information above ~5 kHz offset frequency. The power spectrum of calculated timing jitter is plotted in Fig. 7(a) as orange dots. The timing jitter obtained from the numerical simulation fits well with the experimental data, when assuming the spontaneous emission factor of θ = 3, which is a reasonable number for Er-fiber lasers [19].

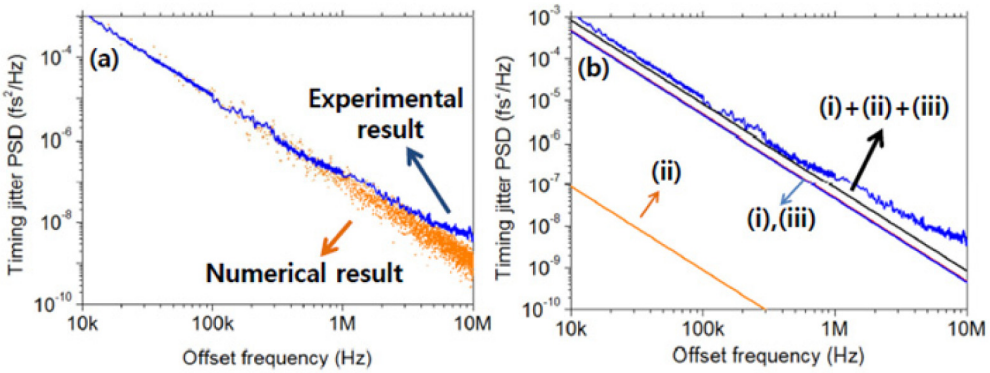

Fig. 7. (a) Numerical timing jitter estimation. (b) Calculated timing jitter by the modified Namiki-Haus noise model. (i) ASE-originated direct timing jitter; (ii) center frequency noise-originated timing jitter coupled by dispersion; (iii) center frequency noise-originated timing jitter coupled by pulse chirp. Blue curve shows the measured result for comparison.

4.2. Analytical modeling based on a modified Namiki-Haus noise model

We also develop analytical modeling to further study the underlying physics in the measured timing jitter performance. For this purpose, the noise model of stretched-pulse fiber lasers developed by S. Namiki and H. Haus [20] is modified in this work. As this model effectively evaluates the timing jitter in fiber lasers in the presence of intra-cavity pulse breathing, we attempted to adopt it for filtered normal-dispersion fiber lasers with a few modifications, while keeping the perturbation analysis for the chirped Gaussian pulse. In our modeling, we modified the bandwidth and chirp parameter terms.

In the case of bandwidth term, the original Namiki-Haus theory assumes that only the gain element stabilizes the spectrum fluctuation. However, due to the use of optical filter in our lasers, the filter bandwidth term should be also included. Effectively, as the filter bandwidth is much narrower than the gain bandwidth in our system, we could replace the gain bandwidth term with the filter bandwidth term, as was also suggested in [26]. Regarding the chirp

#243785 Received 25 Jun 2015; revised 19 Aug 2015; accepted 19 Aug 2015; published 21 Aug 2015

parameter β, it is calculated as $\beta = \tan\{\frac{1}{2}[\arg(\alpha - j) - \arg(\frac{g}{\Omega_g^2} + jD)]\}$, where g is net amplitude gain, D is net cavity dispersion, α is a proportionality factor (self-amplitude modulation coefficient), and Ω_g is gain bandwidth. This equation is based on the symmetry point signature in the cavity of stretched-pulse lasers [20]. However, the symmetry point is broken by the optical filtering in dissipative mode-locked lasers, and this equation cannot be used for modeling our laser. Fortunately, the chirp parameter can be also directly determined from its definition, $\tau = \tau_0\sqrt{1+\beta^2}$, where τ and τ_0 are the actual pulse duration and the transform-limited pulse duration, respectively. In this way, we obtain the chirp parameter for our model as 4.6, which is obtained by the numerical simulation shown in Fig. 6(c).

With these two modifications, we calculate the timing jitter of normal-dispersion Er-fiber lasers with intra-cavity filtering. The spontaneous emission factor θ is set to 3, which is same as the numerical simulation in Section 4.1. The used value of α (self-amplitude modulation coefficient) is 0.2, considering the general range of 0.1-0.3 as shown in [20]. Net amplitude gain of 1.36 is used, which is same as the used value in the numerical simulation. The pulse width and pulse energy are set to 620 fs (FWHM) and 1.1 nJ, respectively, where both are the measured results. Using these parameters, the timing jitter is calculated by Eq. (55) in [20].

The calculated direct ASE-originated timing jitter is shown as curve (i) in Fig. 7(b). Curves (ii) and (iii) represent the center frequency noise-originated timing jitter coupled by intra-cavity dispersion and pulse chirp, respectively. Note that the chirp-coupled, frequency noise-originated jitter (curve (iii)) has a similar magnitude with the direct ASE jitter (curve (i)), and these two contributions mostly determine the overall jitter performance. The contribution from the dispersion (curve (ii)) is negligible due to narrow bandpass filtering.

5. Summary

In this work, we show the accurate timing jitter measurement result of normal-dispersion (+ 0.0084 ps^2) Er-fiber lasers with 9-nm intra-cavity filtering. The measured timing jitter is 3.46 fs (rms) when integrated from 10 kHz to 10 MHz offset frequency. Further, based on measurement of timing jitter spectral density and associated laser parameters, we analyze the jitter spectrum using both numerical simulation and analytical modeling. The numerical simulation shows that adding white Gaussian noise in the SSFT-based pulse dynamics simulation can effectively reproduce the measured jitter spectrum. We also develop an analytical model for filtered normal-dispersion fiber lasers by modifying the Namiki-Haus noise model for chirped Gaussian pulses. With modifications in bandwidth and chirp parameter, the timing jitter is analytically calculated and shows a consistent result with numerical and experimental results. Thus, we anticipate that our numerical simulation and analytical modeling methods can be used to further optimize the timing jitter and other noise of filtered normal-dispersion fiber lasers in the near future.

Acknowledgment

This research was supported by the National Research Foundation (NRF) of South Korea under grants 2012R1A2A2A01005544 and 2013M1A3A3A02042273.

#243785 Received 25 Jun 2015; revised 19 Aug 2015; accepted 19 Aug 2015; published 21 Aug 2015